CUTOFF FREQUENCIES FOR IMPULSE RESPONSE TESTS OF EXISTING FOUNDATIONS

By Sarah L. Gassman,[1] Associate Member, ASCE, and Richard J. Finno,[2] Member, ASCE

ABSTRACT: The impulse response test is a nondestructive evaluation technique commonly used for quality control of driven concrete piles and drilled shafts where the pile heads are accessible. When evaluating existing foundations, the presence of a pile cap or other structure makes the pile heads inaccessible and introduces uncertainties in the interpretation of impulse response results. A test section was constructed at the National Geotechnical Experimentation Site (NGES) at Northwestern University to examine the applicability of nondestructive testing methods in evaluating deep foundations under inaccessible-head conditions. This paper focuses on the results of impulse response tests conducted atop the three pile caps at the NGES. Based on field experimentation and numerical simulations, a frequency was determined below which the impulse response test could be used for inaccessible-head conditions. This cutoff frequency primarily depends upon the geometry of the pile cap and pile. A case study is presented that describes impulse response tests obtained on a number of drilled shafts both after the shaft was constructed and after grade beams and walls were built. The results of these tests also follow the trends observed in the NGES tests related to cutoff frequency.

INTRODUCTION

Nondestructive evaluation (NDE) techniques have been used for a number of years to provide quality control of construction procedures for drilled shafts and driven concrete piles. In particular, sonic echo and impulse response methods have been used extensively to check lengths and continuity of newly installed foundations (e.g., Davis and Dunn 1974; Higgs and Robertson 1979; Hearne et al. 1981; Olson and Wright 1989; Lin et al. 1991). In recent years, the need to evaluate conditions of in-service foundations has arisen as a result of rehabilitation studies of existing structures and the federally mandated inspection of bridges. In some cases, the latter task involves identifying unknown bridge foundation types, because plans for older structures are no longer available. Evaluation of existing foundations differs from the usual methods of NDE in that a structure now covers the tops of deep foundations, and this structure alters the results of an NDE test as compared with one conducted directly atop the deep foundation.

To analyze the applicability of NDE methods to evaluate deep foundations under inaccessible-head conditions in a controlled environment, a test section was constructed at the National Geotechnical Experimentation Site (NGES) at Northwestern University. The test section consists of five drilled shafts constructed with reinforced concrete caps to form three groups of shafts. After the five shafts were constructed, sonic echo and impulse response tests were conducted on each shaft with its top exposed, which is herein called an accessible-head condition. The results of these tests are presented in Finno and Gassman (1998). After the reinforced concrete pile caps were constructed, these tests were again conducted from the tops of the pile caps, which is herein called an inaccessible-head condition.

This paper presents an evaluation of the capabilities of impulse response tests to determine the conditions of drilled shafts under inaccessible-head conditions. To accomplish this goal, construction of the shafts was closely monitored so that the geometries of the shafts could be known with as much accuracy as possible. Because the interpretation of NDE tests of foundations in general is an inverse problem, the tests were numerically simulated to help define the predictive capabilities of the method. This paper briefly describes the NDE test section, presents the results of the inaccessible-head testing at the NGES, compares numerical simulations of the impulse response tests with observed results, defines applicable frequency ranges for which meaningful information can be obtained concerning the deep foundation, presents a case study to illustrate the methods, and presents conclusions regarding the applicability of the test to inaccessible-head conditions.

NDE TEST SECTION

A test section consisting of three groups of drilled shafts was constructed to provide a controlled site where various NDE techniques could be performed to evaluate their applicability for determining the integrity of inaccessible deep foundations. A cross section showing the drilled shafts and the subsurface conditions is given in Fig. 1. As summarized in Table 1, the test section consists of five drilled shafts with lengths between 12.2 and 27.4 m and diameters between 610 and 910 mm. The main variables considered in the test section are the shaft length to shaft diameter ratio (L/D), the pile cap depth to shaft diameter ratio (B/D), and the soil condition at the shaft toe, soft clay, hard silt, or dolomite bedrock. Two of the shafts were purposely constructed with defects, a reduced cross section (neck) in shaft 2 and a thin, soil-filled joint in shaft 1. These defects represent typical construction deficiencies that can occur when temporary casing is pulled as concrete is placed in a shaft. Sixty cylinders were made from the concrete as it was placed to determine strength and propagation velocity variations over time.

TESTING EQUIPMENT AND PROCEDURES

The impulse response method is a surface reflection technique that relies on the identification of compressive wave reflections to evaluate shaft integrity. The test involves impacting the top of a drilled shaft with an impulse hammer, which induces transient vibrations. Both the impact force and particle velocity are measured on the impacted surface. Particle velocity is recorded in the time domain with a geophone, and the signal is digitally converted to the frequency domain fro analysis.

The testing setup for accessible- and inaccessible-head tests

[1]Asst. Prof., Dept. of Civ. and Envir. Engrg., Univ. of South Carolina, Columbia, SC 29208.

[2]Prof., Dept. of Civ. and Envir. Engrg., Northwestern Univ., Evanston, IL 60208.

Note. Discussion open until July 1, 2000. To extend the closing date one month, a written request must be filed with the ASCE Manager of Journals. The manuscript for this paper was submitted for review and possible publication on July 23, 1999. This paper is part of the ***Journal of Performance of Constructed Facilities***, Vol. 14, No. 1, February, 2000. ISSN 0887-3828/00/0001-0011–0021/$8.00 + $.50 per page. Paper No. 21476.

TABLE 1. NDE Test Section Details

Shaft (1)	Length, L (m) (2)	Diameter, D (mm) (3)	Cap Height, B (mm) (4)	L/D (5)	B/D (6)	Comments (7)
1	12.2	610	610	20	1	Soil-filled joint
2	21.3	914	610	23.3	.67	Reduced cross section
3	12.2	610	1,524	20	2.5	—
4	21.3	762	914	28	1.2	—
5	27.5	914	914	30	1	—

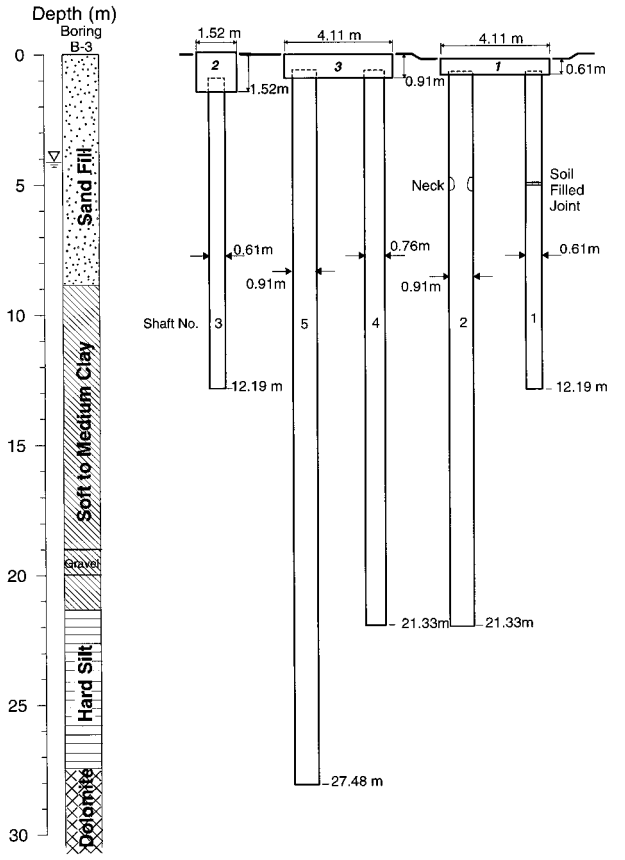

FIG. 1. Cross Section of NGES Deep Foundation Test Section

is schematically shown in Fig. 2. The equipment used for these tests includes a portable computer equipped with a data acquisition board and signal conditioning card, an impulse hammer, and a geophone. The portable PC is used for acquiring, analyzing, and storing the data. The impact hammer is equipped with a load cell and is capable of generating transient vibrations with frequencies as high as 2,000 Hz. Vibrations at the shaft head are recorded by a vertical geophone that is activated upon hammer impact by means of a triggering device in the portable PC to which both the hammer and geophone are connected. The data acquisition rate for this work was 10,000 points/s.

The tests on the inaccessible shafts were conducted by impacting the pile cap directly above the center of each shaft. The vibrations were recorded with a geophone mounted to the pile cap surface just outside the perimeter of the projection of a shaft. This geophone location minimized reflections from the pile cap while capturing reflections from the toe of the shaft (Gassman 1997). The inaccessible-head tests were performed 19 days after the pile caps were constructed. This was 74–77 days after the drilled shafts were cast.

The data analysis is conducted in the frequency domain, although the velocity-time data acquired during the test can also be analyzed as a sonic echo test. A fast Fourier transform is performed on both the force and the velocity signals. The resulting velocity spectrum is divided by the force spectrum to give the mobility as a function of frequency. Various filtering techniques may be used to remove noise from the data at frequencies that obscure identification of significant reflections. For this study, results from several hammer blows were averaged to obtain input to the mobility plots. The mobility data was filtered by applying a lowpass Blackman window, which smoothed fluctuations in the mobility plot.

An idealized mobility versus frequency plot is shown in Fig. 3. Quantitative information concerning the shaft length and impedance can be obtained from this plot. Because of a shaft's cylindrical shape, theory of elasticity indicates that a prismatic deep foundation has a constant frequency spacing between resonant peaks. This frequency is a function of the shaft length and propagating wave velocity if the induced wave lengths are greater than the diameter of the shaft. By measuring the frequency change, Δf, between resonant peaks, the length from the geophone to the source of the reflection, L, can be found from

$$L = \frac{v_c}{2\Delta f} \tag{1}$$

where v_c = propagation (bar) velocity in concrete and can be expressed as $v_c = \sqrt{(E/\rho_c)}$, where E = Young's modulus and ρ_c = density of concrete. As the concrete cures, its strength and stiffness increase. In practice, v_c = 4,000 m/s is indicative of ''good'' quality concrete, although a range of 3,500–4,500 m/s has been used by various authors (e.g., Davis and Robertson 1975; Hearne et al. 1981).

The shaft mobility, N, is the inverse of the shaft impedance. It is theoretically defined (Davis and Robertson 1975; Stain 1982) as

$$N = \frac{1}{\rho_c v_c A} \tag{2}$$

where A = cross-sectional area of the shaft. It can be experimentally found by taking the geometric mean of the maximum height, P, and the minimum height, Q, of the resonant peaks in the portion of the mobility curve where the shaft response is in resonance, and it is equal to

$$N = \sqrt{PQ} \tag{3}$$

If the actual N is greater than the theoretical value, it is likely that there is a defect in the shaft, perhaps due to a smaller than anticipated cross section (i.e., a neck) or poor concrete quality (low ρ_c or v_c).

Resolution of impulse response signals can be defined by the ratio P/Q. When P/Q approaches 1.0, no resonant frequencies can be identified; thus, one cannot expect to locate the bottom of a shaft under those conditions. Higher signal resolution makes the resonant peaks easier to distinguish and thus makes it easier to interpret pile length and location of anomalies.

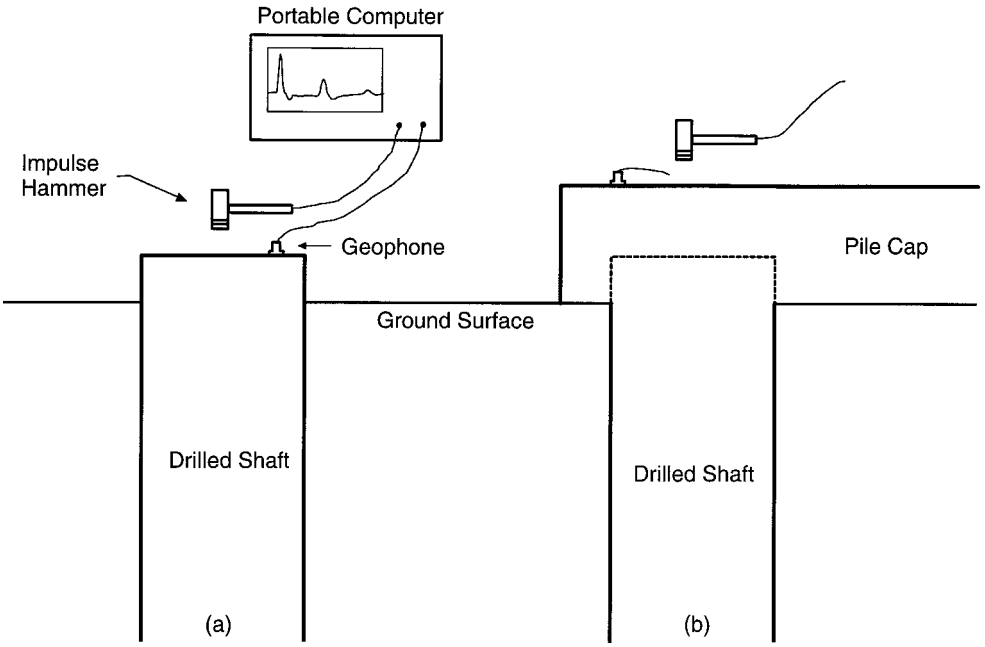

FIG. 2. Schematic of Impulse Response Testing Equipment and Testing Configuration: (a) Accessible-Head Condition; (b) Inaccessible-Head Condition

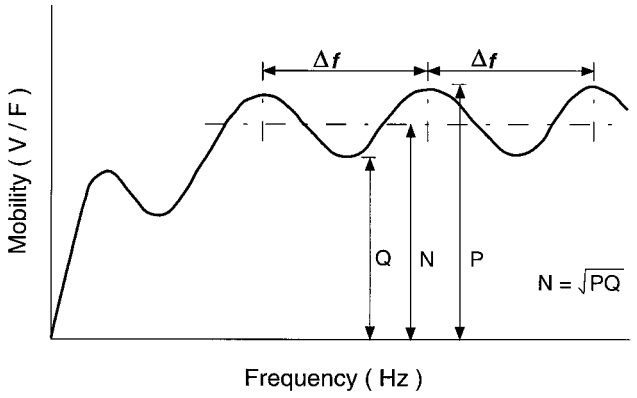

FIG. 3. Ideal Mobility Plot

RESULTS OF TESTING AT NDE TEST SECTION

Impulse Response Results: Shafts without Planned Defects

The results for the inaccessible-head tests performed on shaft 3 are shown in Figs. 4 and 5. The accessible-head results obtained 28 days after shaft 3 was constructed are also shown for comparison. The pile cap is 1.52 m long, 1.52 m wide, and 1.52 m high. The distance between the top of the cap and the top of the shaft is 0.72 m; thus, the total length of the shaft and cap is 12.9 m. As shown in Fig. 4(a), the input force for the inaccessible test has a larger magnitude and a shorter contact time than the accessible test, resulting in a broader frequency range, as shown in Fig. 4(c). According to Sansalone and Carino (1986), significant energy is imparted at frequencies below the inverse of the contact time of an impulse loading. For contact times of 0.9 and 1.1 ms, these frequencies are 1,100 and 900 Hz for the inaccessible- and accessible-head tests, respectively. When evaluating mobility data, the regions where results can be reliably considered are those where frequencies are lower than these frequencies, because mobility is defined as velocity divided by force and errors (i.e., noise in a signal) in relatively low force input can result in large errors in mobility. The larger amplitude of force in the inaccessible-head test was needed to provide enough energy to penetrate through the cap, reach the shaft toe, and reflect back to the cap surface.

Comparison of the velocity-time traces for the accessible and inaccessible cases, shown in Fig. 4(b), indicates that the interpretation of the velocity-time signal alone, as is done with the sonic echo test, requires considerable judgment for the inaccessible case. The toe reflection for shaft 3 in the accessible condition was strong and clear, and analysis of the shaft length was straightforward. For the inaccessible-head test, reflections from a combination of the pile cap boundaries and surface waves generated by the impact are identified in the velocity-time trace, spaced at 0.83 ms. These reflections govern the response and mask reflections arriving from the shaft toe. Therefore, the velocity spectrum shown in Fig. 4(d) is better suited to analyze shaft 3 in the inaccessible condition, and it indicates several trends. For frequencies lower than 600 Hz, reflections from the bottom of the shaft cause low resolution resonances in the inaccessible-head tests. There also is a strong resonance at 1,200 Hz caused by a combination of reflections from the interface between the bottom of the pile cap and the shaft, and reflections from the waves reflecting from the ends of the caps.

The mobility plots for both the accessible- and inaccessible-head tests are shown in Fig. 5(a); for clarity, the lower frequency portion of the inaccessible test is shown on an expanded scale in Fig. 5(b). As shown, reflections from the shaft toe are apparent for both accessible and inaccessible conditions, although the resonances for the inaccessible case were significantly less pronounced than the accessible case. This is because little signal is transmitted past the pile cap into the shaft due to the impedance difference between the pile cap and the drilled shaft. The most notable difference for the inaccessible case is the character of the low frequency portion of the curve. In contrast to the constant magnitude of the resonating peaks up to 1,000 Hz for the accessible case, the peaks in the inaccessible case exponentially decrease between 100 and 600 Hz and are not identifiable beyond 600 Hz. Therefore, the pile cap reduced the frequency range for which usable information concerning the entire length of the shaft could be obtained.

Comparison of the accessible and inaccessible cases indicates several trends in the mobility signals. The average mo-

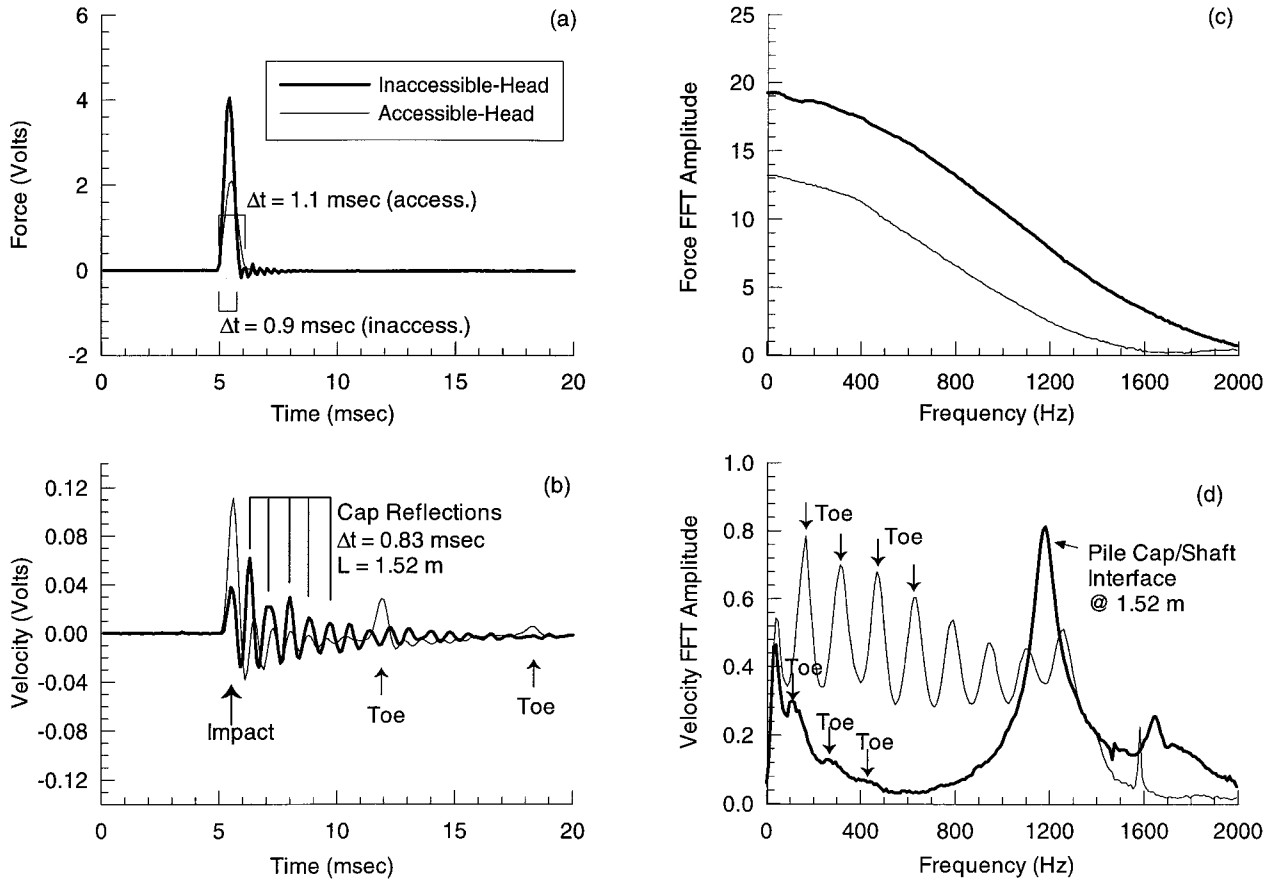

FIG. 4. Force and Velocity Responses for Shaft 3 with Pile Cap: (a) Force-Time Trace; (b) Velocity-Time Trace; (c) Force Spectrum; (d) Velocity Spectrum

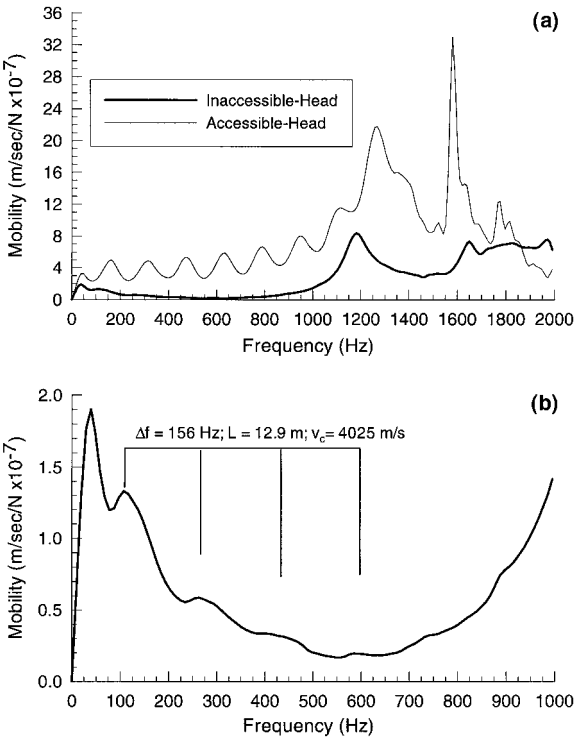

FIG. 5. Mobility Plot for Shaft 3 with Pile Cap: (a) Accessible and Inaccessible Results up to 2,000 Hz; (b) Inaccessible Results up to 1,000 Hz

bility decreased from 3.8×10^{-7} m/s/N for the accessible case to 0.5×10^{-7} m/s/N for the inaccessible case, as expected due to the increased mass from the pile cap. Another notable difference between the two mobility curves is the rise in the inaccessible-head mobility signal that develops around 1,200 Hz. This rise is caused by both the strong reflection from a depth of 1.52 m at the bottom of the pile cap and reflections from the surface waves off the pile cap boundaries. For the inaccessible case, the resolution, P/Q, was 1.2 at frequencies below 600 Hz, whereas that of the accessible-head condition was 1.9 for frequencies as high as 1,000 Hz.

Impulse Response Results: Shafts with Planned Defects

Shaft 2 was constructed with a planned necking defect located 4.95 m from the top of the pile cap. The total length of the shaft and cap is 21.8 m. Its pile cap is 4.11 m long, 1.52 m wide, and 0.61 m thick. The force impact imparted significant force up to frequencies of about 1,100 Hz. Fig. 6(a) compares the velocity-time traces and indicates that reflections from the neck defect are clear for both cases around 8 ms, but the reflection from the shaft toe at 16.7 ms is not clear in the inaccessible-head case. As observed in the velocity spectrum in Fig. 6(b), the reflection from the neck observed at 8 ms in the velocity-time trace corresponds to the resonance around 420 Hz, yet multiples of this resonance are not apparent in either the time trace or the frequency spectrum for the inaccessible-head test. Four clear resonating peaks below 500 Hz from the shaft toe are clear for both the accessible and inaccessible cases. The three larger, broader resonances observed between 400 and 1,600 Hz in the accessible-head case, which reflect the neck response, are observed in the inaccessible-head

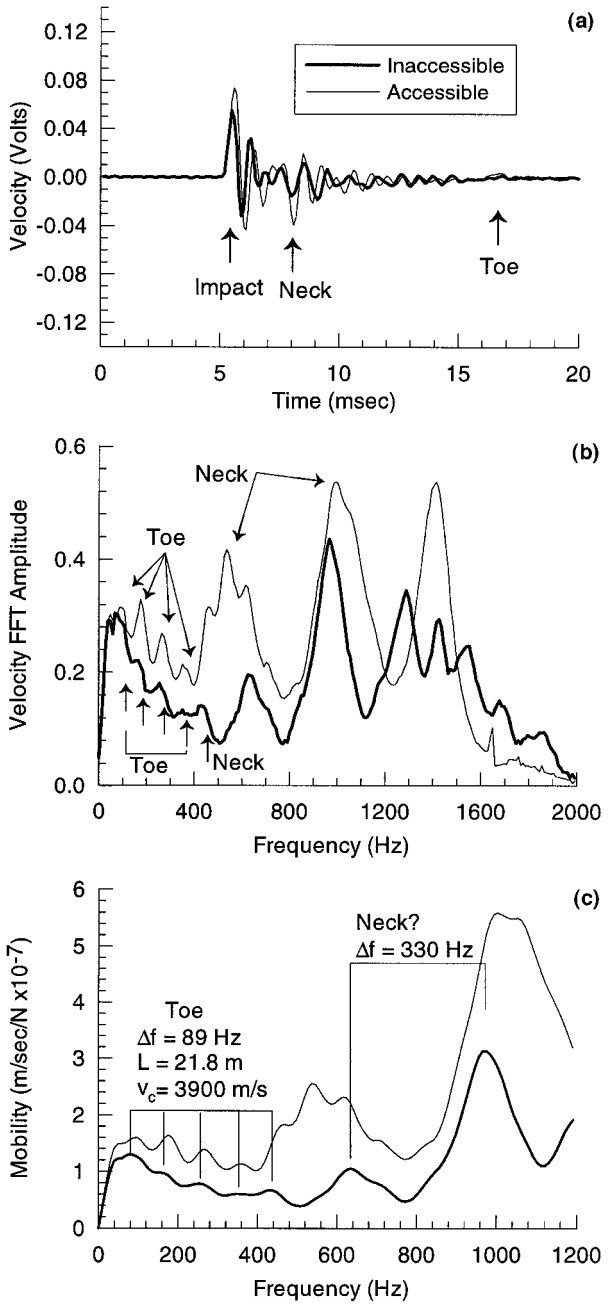

FIG. 6. Impulse Response for Shaft 2 with Pile Cap: (a) Velocity-Time Trace; (b) Velocity Spectrum; (c) Mobility Plot

case between 600 and 1,300 Hz. However, the peaks are not equally spaced in the latter, suggesting that these and the resonances above 1,400 Hz originate from, or are affected by, wave reflections from the sides of the pile cap.

Comparison of the mobility signals in Fig. 6(c) indicates that the toe of shaft 2 was detected for test with and without the pile cap atop the shaft, although the resonances for the inaccessible case were less pronounced than for the accessible case. A strong signal reflected from both the neck defect and the bottom of the cap in the inaccessible case, leaving less energy to be transmitted down the full length of the shaft, and resulted in a less distinct resonance.

Five resonating peaks from the shaft toe are clearly visible at frequencies below 500 Hz in the inaccessible-head result, compared with nine resonances below 800 Hz in the accessible-head result. The average change in frequency between these peaks is 89 Hz and for a total shaft and cap length of 21.8 m, the propagation velocity, v_c, computed from (1) is 3,900 m/s. The reflection from the neck that was clearly identifiable by peaks at 540 and 1,000 Hz in the accessible-head response may be seen in the inaccessible result by the peaks at 620 and 960 Hz. This corresponds to a change in frequency equal to 330 Hz. It might be interpreted that these resonances originated from the neck located 4.95 m below the cap surface. However, the calculated propagation velocity of 3,270 m/s from (1) (Δf = 330 Hz and L = 4.95 m) is less than the 3,900 m/s determined from the five resonating peaks below 500 Hz. It is likely, therefore, that these resonances are affected by surface wave reflections from the sides of the pile caps and do not emanate solely from the neck.

The presence of the pile cap atop shaft 2 created a decrease in the average mobility from 1.2×10^{-7} m/s/N to 0.7×10^{-7} m/s/N and a decrease in resolution, P/Q, from 1.3 to 1.2 for the resonances from the shaft toe. The resonances from the defect also exhibited a decrease in mobility and resolution.

Tests above Center of Pile Cap

Impulse response tests were conducted by placing the geophone and impacting the hammer at locations on the pile cap away from the drilled shafts to quantify the response of the pile cap alone. One typical result, performed on pile cap 1 between shafts 1 and 2, is presented in Fig. 7. This test was performed by striking the hammer in the center of the pile cap and placing the geophone 460 mm from the center position, along either the short or the long axis. The tests performed on both axes are shown, as are the tests performed directly above shaft 2. Comparison of these tests indicates a significantly different response. Resonances from the toe of the shaft are seen for the test above the shaft, whereas the tests in the center of the cap are characterized by a broad peak of higher mobility occurring around 200 Hz with no resonances from the toe of the shaft. Also, the responses from the short and long axis geophone locations deviate around 450 Hz, as a result of the cap boundaries. The length of the short axis is 1.52 m and that of the long axis is 4.11 m. Placing the geophone on the shorter axis, closer to an edge, resulted in stronger resonances between 450 and 1,000 Hz.

Information concerning the inaccessible-head condition can also be obtained by examining the higher frequency portion of the velocity spectrum, because meaningful responses in terms of mobility are limited by the contact time of the hammer strike. At these higher frequencies, resonant frequencies corresponding to the shallow depths of the structural interfaces can be identified. This is best illustrated by examining the velocity spectrum for the inaccessible-head test on shaft 3, shown in Fig. 4(d), which showed a strong single resonance at 1,200 Hz. This corresponds to a reflection from a depth of 1.52 m at the bottom of the pile cap for a propagation velocity of 3,700 m/s. This propagation velocity is less than the 4,080 m/s determined by using the correlation from unconfined compression strength for the cylinders cast from the concrete of

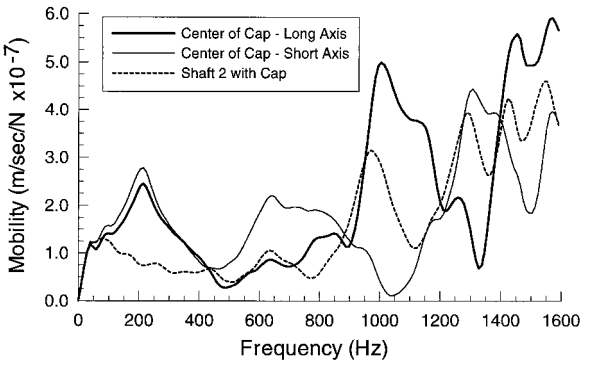

FIG. 7. Center of Pile Cap Test for Pile Cap 1

TABLE 2. Summary of Accessible- and Inaccessible-Head Impulse Response Results

Shaft number (1)	L/D ratio (2)	B/D ratio (3)	Average Mobility, N (m/s/N E-7)			Resolution, P/Q	
			Accessible (4)	Inaccessible (5)	Theoretical[a] (6)	Accessible (7)	Inaccessible (8)
1	20	1	6 (defect) 1.6 (toe)	1.0	3.6–4.1	9 1.2	2.5 1.1
2	23.3	0.67	3 (defect) 1.2 (toe)	0.7	1.4–1.8	2.8 1.3	2.1 1.2
3	20	2.5	3.8	0.5	3.6–4.1	1.9	1.13
4	28	1.2	1.9	0.6	2.0–2.63	1.2	1.0
5	30	1	1.4	0.5	1.4–1.8	1.05	1.0

[a] v_c = 3,500 to 4,500 m/s; ρ_c = 2,400 kg/m^3.

the pile caps, tested for a 28 day strength (Gassman 1997). However, these inaccessible-head tests were performed 19 days after concrete placement; thus, a lower propagation velocity may be expected and a value of 3,700 m/s is not unreasonable.

Given the limits of the impulse hammer used for this study, which input frequencies up to 2,000 Hz, the interfaces between the cap and the shaft for pile caps 1 and 3 were not detected by examining the velocity spectrum. A strong resonance is expected around 3,350 and 2,250 Hz for pile caps 1 and 3, respectively, based upon a propagation velocity of 4,080 m/s. These resonant frequencies are greater than 2,000 Hz, the upper limit induced by the impulse hammer; thus, resonances from the bottom of the pile cap were not seen in the velocity spectrum [e.g., Fig. 6(b)].

Summary of Effects of Intervening Structure

The analyses of the accessible and inaccessible results are summarized in Table 2. The presence of the pile cap had two notable effects on the results. For all five shafts tested, both the average mobility and the resolution decreased. These two effects are attributed to the pile cap, which increased the mass of the system. The cap creates an impedance change at the interface between the cap and the shaft which causes an incident wave to reflect, resulting in less energy being transmitted down the shaft. The response for the inaccessible-head tests is characterized in the mobility plot by peaks that follow an exponentially decreasing trend in the lower frequency region, in contrast to the more constant magnitude of the resonating peaks for the accessible-head tests. The responses of the inaccessible tests can also be considered in light of the transition from a one-dimensional wave propagation in a drilled shaft to a more complicated, three-dimensional response arising from the geometry of a pile cap. Unlike the accessible-head tests, where the induced wavelengths are greater than the shaft diameter, the wavelengths at higher frequencies are smaller than the pile cap dimensions, which leads to deviations from the conditions of normally-assumed 1D wave propagation.

The results of the accessible- and inaccessible-head impulse response tests defined the limits of the method for the conditions at the Northwestern NGES. Using the methods on shafts obscured by pile caps, the toes of shafts 1, 2, and 3 were identified ($P/Q > 1$ in Table 2), whereas the toes of shafts 4 and 5 were not ($P/Q = 1$). This can be explained by the L/D and B/D ratios for each shaft, as well as the surrounding soil conditions. Shafts 4 and 5 had L/D ratios of 28 and 30, both of which are near the limits of the conventional testing method (Davis and Robertson 1975), and B/D ratios of 1.2 and 1, respectively. The three shafts in which the toe was identified had L/D ratios of 20, 23, and 20 for shafts 1, 2, and 3 and B/D ratios of 1, 0.67, and 2.5, respectively. These three shafts have similar L/D ratios, but shaft 3 has the largest B/D ratio. The B/D ratios for shafts 4 and 5 are in the middle of the ratios tested for this study. Therefore, the limits of the impulse response method for detecting the toe of a shaft with a pile cap are a combination of the L/D ratio and B/D ratio, as well as the soil conditions adjacent to a shaft. At the NGES, the toe of the shaft could be identified for inaccessible shafts with L/D ratios as high as 23 with a B/D ratio of 0.67 and with L/D ratios as high as 20 with a B/D ratio of 2.5. Both defects, the soil-filled joint in shaft 1 and the neck in shaft 2, were identified in the inaccessible-head tests for B/D ratios of 1 and 0.67, respectively.

NUMERICAL SIMULATION OF NGES INACCESSIBLE SHAFTS

Numerical simulations of the impulse response tests were conducted with the Siminteg Simulation Program developed by CEBTP of France (Paquet 1968) and revised by STS Consultants, Ltd. (Davis 1994). The program is based on impedance relationships between the properties of the pile and the surrounding soil. To simulate a result from an impulse-response test, a pile or drilled shaft is modeled as a cylinder surrounded by infinitely extending horizontal soil layers. The pile is divided into as many as ten segments and a base. Each pile segment is assigned a length, diameter, concrete propagation velocity, and density. A shear wave velocity and density are assigned for the soil surrounding each segment.

The first step in the model is to calculate the impedance for the pile base for the prescribed frequency range associated with the impulse hammer impact. This calculation considers a spring on an elastic base and assigns the pile base the same diameter as the bottom segment and assumed to be on the ground surface, i.e., a plate on the ground. For each of the pile segments, from the top of the pile downwards, several parameters are calculated. A general damping coefficient (Paquet 1968) is calculated by combining the various damping coefficients for the pile and soil. The impedance of each segment is calculated, and the energy lost for each segment is accounted for by the geometry of the shaft and the damping properties of the soil, respectively. The variation of impedance with frequency is then calculated by looping over the number of segments. At the end of each segment in the loop, the effect of the impedance from the present segment is added to the impedance from the previous calculations in the form of a complex array representing the variation of impedance with frequency. The inverse of the magnitude of the complex entry of this summed array at the end of the loop is the simulated mobility for the pile.

This simulation program is based on one-dimensional analysis of a cylindrical rod and, as such, is strictly valid for only axisymmetric conditions. Simulations for each inaccessible shaft were based on the best fit parameters used to match the response of the accessible-head tests (Finno and Gassman 1998) and the as-built lengths given in Table 1. These simulations are approximations of the actual conditions, because two of the three pile caps are rectangular; thus, the pile cap-

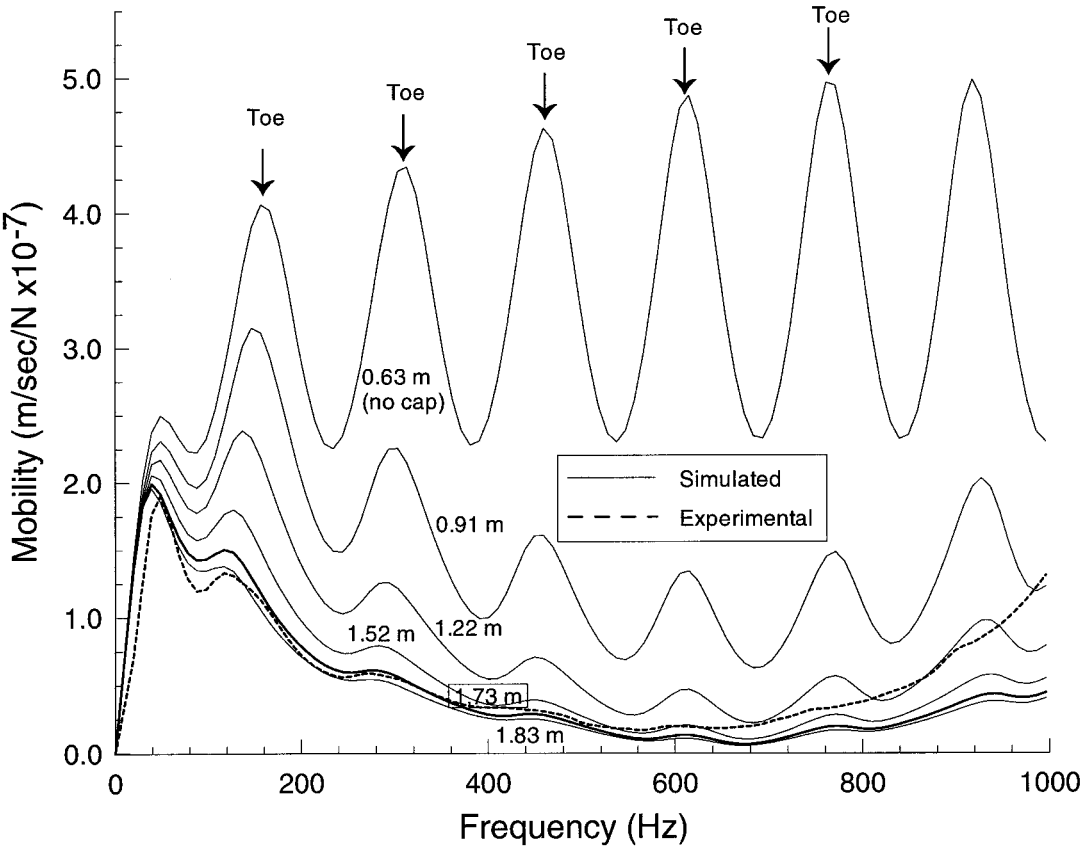

FIG. 8. Numerical Simulation of Shaft 3 with Varying Pile Cap Diameter

shaft system is not axisymmetric. The cap geometry was converted to an ''equivalent'' cylinder by determining an ''effective'' diameter for each cap by modeling the shaft with the best-fit parameters from the accessible shaft simulations and adding a concrete cylinder of variable radius. The radius of the cylinder was increased until good agreement was found between the experimental and simulated mobility curves.

Shaft 3

Pile cap 2, atop shaft 3, was modeled as a cylinder with a depth of 1.52 m and a diameter varying from 0.63 to 1.83 m. The results for the simulated responses from each diameter are shown in Fig. 8. As the simulated diameter of the cap was increased, the resolution of the peaks decreased and the average mobility of the signal decreased exponentially between frequencies of 60 and 700 Hz. The best match of the simulated and observed signals was achieved with a pile cap diameter of 1.73 m, at least up to about 600 Hz, where the two signals began to diverge. Both these signals identified four resonating peaks below 600 Hz with similar resolution and average mobility. Based on the best-fit diameter of 1.73 m, the effective area for cap 2 is determined to be 2.34 m^2, essentially equal to the as-built area of the pile cap of 2.32 m^2. This agreement should be expected, because the square cap was essentially axisymmetric and was thus well modeled in the one-dimensional simulation.

Shaft 2

Fig. 9 shows the results of the simulations of shaft 2 below cap 1. The pile cap was modeled with a depth of 0.61 m and a range of diameters from that of the shaft up to 2.75 m. As the diameter of the pile cap was increased, the resolutions of the resonances corresponding to the toe and the defect decreased, as did the average mobility. For an effective diameter of 2.29 m, a good match between the simulated and the observed signals was achieved up to 460 Hz. Three resonances from the shaft toe below 400 Hz and one resonance from the defect at 420 Hz were observed in the simulation. Only the first resonance from the neck defect was matched, because the experimental curve deviated from the simulated curve around 460 Hz. The difference between the experimental and simulated curves at 460 Hz is believed to have been caused by reflections of surface waves that arise from the rectangular geometry of the pile cap, which was not possible to simulate in this axisymmetric approximation. The resonances seen in the experimental result above 460 Hz can therefore be attributed to the actual rectangular geometry of the pile cap not accounted for in the axisymmetric approximation of the cap, the surface wave reflections from the edges of the pile cap, or, more likely, a combination of the two.

The pile cap response was best modeled with an effective diameter of 2.29 m. This diameter corresponds to an equivalent area of approximately half the pile cap contributing to the response for each shaft. For cap 1, the tributary area of the pile cap above each shaft had a width, W_{trib}, equal to 1.52 m and a length, L_{trib}, equal to 2.06 m. Thus, the tributary area is 3.14 m^2, which is less than the effective area of 4.1 m^2 determined for the effective diameter of 2.29 m from the simulations. The ratio of the tributary area to the effective area is equal to 0.76.

FREQUENCY RANGES FOR INACCESSIBLE-HEAD CONDITIONS

For a given pile cap geometry, the effective area, A_{eff}, of a cap can be determined by applying a factor, F, to the calculated tributary area, A_{trib}, of the pile cap atop a shaft:

$$F = \frac{A(\text{tributary})}{A(\text{effective})} = \frac{A_{trib}}{A_{eff}} \tag{4}$$

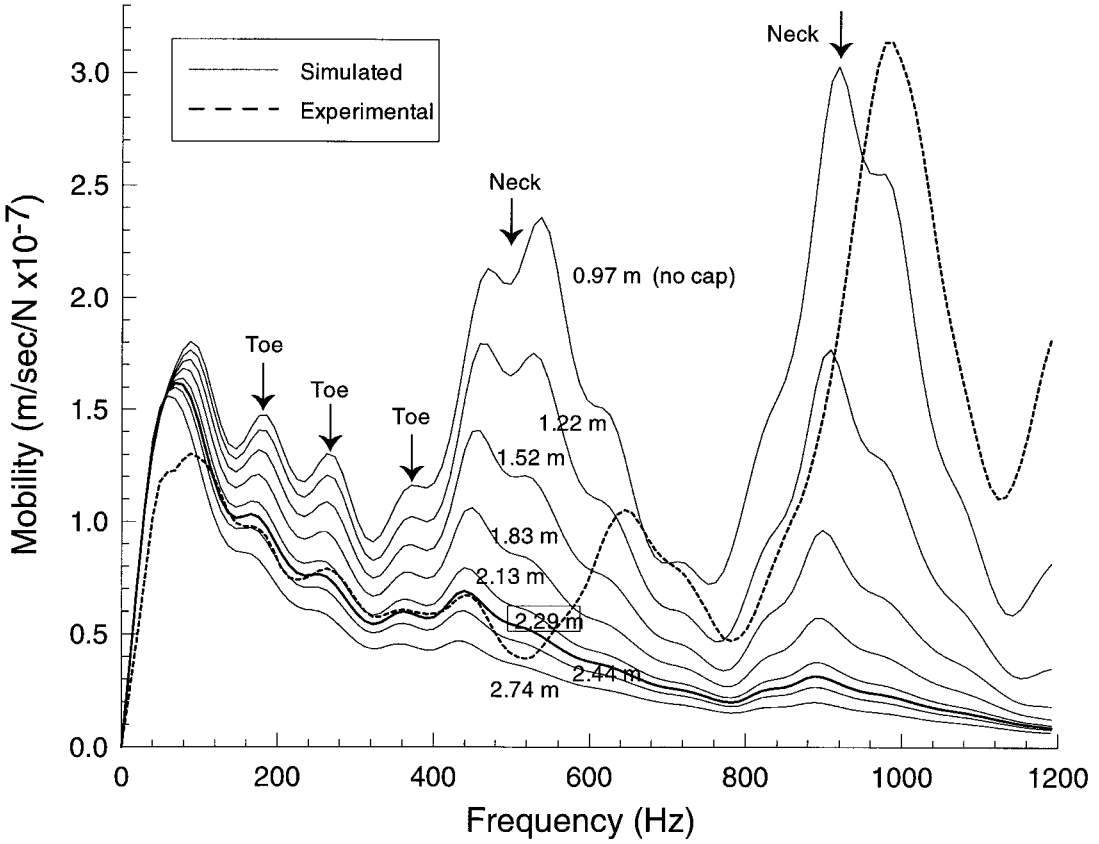

FIG. 9. Numerical Simulation of Shaft 2 with Varying Pile Cap Diameter

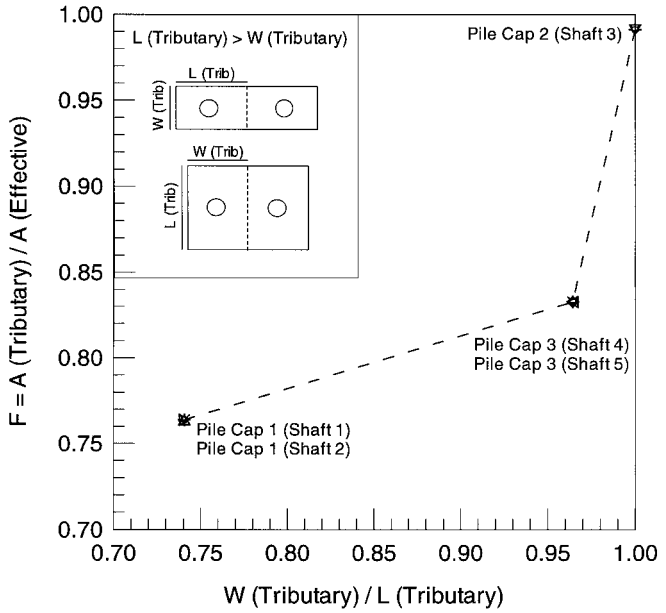

FIG. 10. Shape Factor to Determine ''Effective'' Area from Tributary Area of Pile Cap

A_{trib} is defined as the tributary width, W_{trib}, multiplied by the tributary length, L_{trib}; where L_{trib} is the greater dimension, as shown in Fig. 10. F was determined from the simulations of the three NGES pile caps. The relationship between F and the ratio of the tributary width to the tributary length, W_{trib}/L_{trib}, is shown in Fig. 10. As W_{trib}/L_{trib} approaches 1.0, F approaches 1.0; thus, a square pile cap atop a single shaft yields a geometry that is essentially axisymmetric, as shown for Shaft 3. As the shaft become more rectangular, the effective area increases relative to the actual tributary area.

Analysis of shafts in accessible-head conditions are based on the assumption of one-dimensional wave propagation that occurs when the wavelength of a longitudinal stress wave is greater than or equal to the diameter of the pile. For shafts with diameters between 610 and 910 mm and v_c = 4,000 m/s, the upper bound frequencies needed to maintain one-dimensional conditions vary from 4,400 to 6,560 Hz. Because the impulse hammer used herein imparts frequencies no higher than 2,000 Hz, one-dimensional conditions are maintained for the accessible-head tests.

However, the larger areas created by the pile caps in the inaccessible-head tests will limit the frequencies at which information can be extracted concerning an underlying drilled shaft. This ''cutoff'' frequency can be identified by comparing the experimental and simulated mobility curves. It is postulated that this frequency can be identified as that where the *trends* of an experimental mobility curve diverge from the corresponding simulated curve, because the simulation is based on one-dimensional wave propagation, which does not consider surface wave or three-dimensional effects. Just a simple separation of the simulated and experimental mobility curves is believed to be insufficient to define the cutoff frequency, since other factors may be responsible for the differences in behavior. For example, in Fig. 9, the cutoff frequency can be identified as about 520 Hz, the point when the mobility in the experimental curve has a local minimum while that of the simulated curve continues to decrease. The cutoff frequencies identified in this way for all shafts are summarized in the f_c^2 column in Table 3.

This data was evaluated to develop a relation that can be used to identify the approximate cutoff frequency, f_c, based on geometric relations and the concept that one-dimensional conditions are satisfied when the wavelength is greater than or

TABLE 3. Cutoff Frequencies for Inaccessible Tests

Shaft (1)	B/D (2)	D (m) (3)	A_{eff} (m^2) (4)	α_s (5)	α_t (6)	v_c (m/s) (7)	f_c^1 (Hz) (8)	f_c^2 (Hz) (9)
1	1.0	0.61	4.11	14.05	2	3,876	396	460
2	0.67	0.91	4.11	6.31	1.67	3,960	545	520
3	2.5	0.61	2.34	8.01	3.5	3,950	563	630
4	1.2	0.76	5.27	11.61	2.2	4,100	391	440
5	1.0	0.91	5.27	8.1	2	3,950	430	460

Note: f_c^1 = computed from (5); f_c^2 = based on differences from simulated and experimental results.

equal to the diameter of the shaft. The following relation is proposed:

$$f_c = \frac{v_c}{\lambda_c} \approx \frac{v_c}{D_{\text{eff}}} = \frac{v_c}{D(\alpha_s + \alpha_t)} \tag{5}$$

where λ_c = wavelength where wave propagation in a cylindrical rod is no longer one-dimensional; D_{eff} = effective diameter of the pile cap–shaft system as determined by matching simulations with test data; D = diameter of the shaft; α_s = factor to account for the plan area of the pile cap relative to the area of the shaft; and α_t = factor to account for the relative thickness of the pile cap. These factors are defined as

$$\alpha_s = \frac{A_{\text{eff}}}{\left(\frac{\pi D^2}{4}\right)}; \quad \alpha_t = \left(1 + \frac{B}{D}\right) \tag{6}$$

where B = thickness of the pile cap. It is proposed to limit F in Fig. 10 to 0.75 for W/L ratios below 0.75.

In the limit, the cap thickness goes to zero, α_t goes to 1. As the tributary area of the shaft approaches that of the shaft, α_s goes to 1. As the tributary area gets large relative to the area of the shaft, α_s gets large, which makes the effective diameter of the shaft large and thus makes the cutoff frequency approach 0. As the cutoff frequency gets small, resonances from the shaft toe will be masked by three-dimensional effects. Of these two correction factors, α_s is generally larger and thus has larger impact on the cutoff frequency. Of course, the limitations related to the L/D ratio of a shaft, the soil stratigraphy, and the shear wave velocity of the soil provide additional constraints on the applicability of the method (Finno and Gassman 1998).

The cutoff frequencies computed from (5) and the corresponding parameters for the five shafts are given in the f_c^1 column in Table 3. The propagation velocities, v_c, are those from the best-fit simulations of the accessible head tests (Finno and Gassman 1998). A comparison of the frequencies found by the empirical equation and those determined by comparing the mobilities of the simulations and the experimental curves are shown in Fig. 11. The agreement is reasonably good, and, most importantly, the trend in the empirically predicted data agrees with that of the experimentally derived data.

Case Study

Drilled shaft construction at a building site in Chicago, Illinois, provided an additional opportunity to obtain signals on drilled shafts at times when a shaft was both accessible and inaccessible. These data are presented to show the applicability of the frequency cutoff relation of (5) for inaccessible conditions other than those at the Northwestern NGES.

The subsurface conditions are typical of the downtown area of Chicago and consist of, in descending order, a surficial fill (7.6 m), a hard, desiccated clay layer (5.2 m), a soft to medium clay stratum (3 m), and a hard clay and silt till stratum (7.6 m) overlying dolomite bedrock. The drilled shafts were 0.9 to

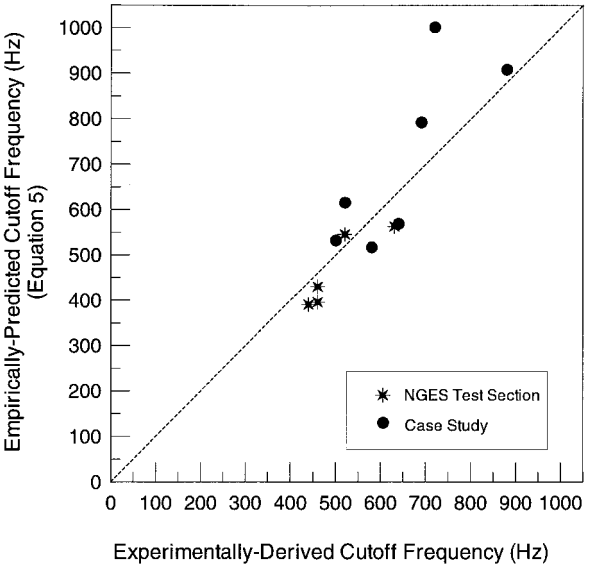

FIG. 11. Cutoff Frequency Empirical Relation

2.4 m in diameter and were belled in the hard clay and silt stratum. The upper part of the drilled shafts were larger than the lower section as a result of the temporary casing used to stablize the surficial deposits.

Seven shafts were tested both after the shaft was constructed and after the additional structure was completed. The L/D ratio of these shafts varied from 10 to 18. After construction of the additional structure, as much as 3.3 m of concrete existed between the top of the concrete cap and the top of the drilled shaft. The B/D ratio varied from 0.7 to 2.9.

To illustrate the results obtained at this site, the mobility versus frequency plot for typical accessible- and inaccessible-head conditions are shown in Fig. 12. The resonant peaks are seen at frequencies less than 800 Hz for the accessible and the inaccessible conditions; however, a deviation from constant amplitude mobility peaks occurs around 400 Hz for the inaccessible case, as a result of reflections from the pile cap boundaries. As was the case for the NGES shafts, the pile cap reduced the frequency range wherein constant amplitude resonances from the toe of the shaft could be identified. Assuming a propagation velocity of 4,000 m/s, shaft lengths corresponding to these peaks are 17.3 and 21.2 m for the accessible and inaccessible conditions, respectively, as compared with the as-built values of 18.1 and 21.4 m. No defects were evident in the construction records.

Numerical simulations were made for each of the seven shafts shown in Table 4 so that the cutoff frequency relation developed for the NGES test section could be evaluated under different conditions. The cutoff frequency was defined based on the differences between the simulated and experimental results in the same manner as previously discussed for shafts 3 and 2. The cutoff frequency was also computed based on the relationship developed at the NGES test section and the parameters shown in Table 4. The pile caps above each shaft

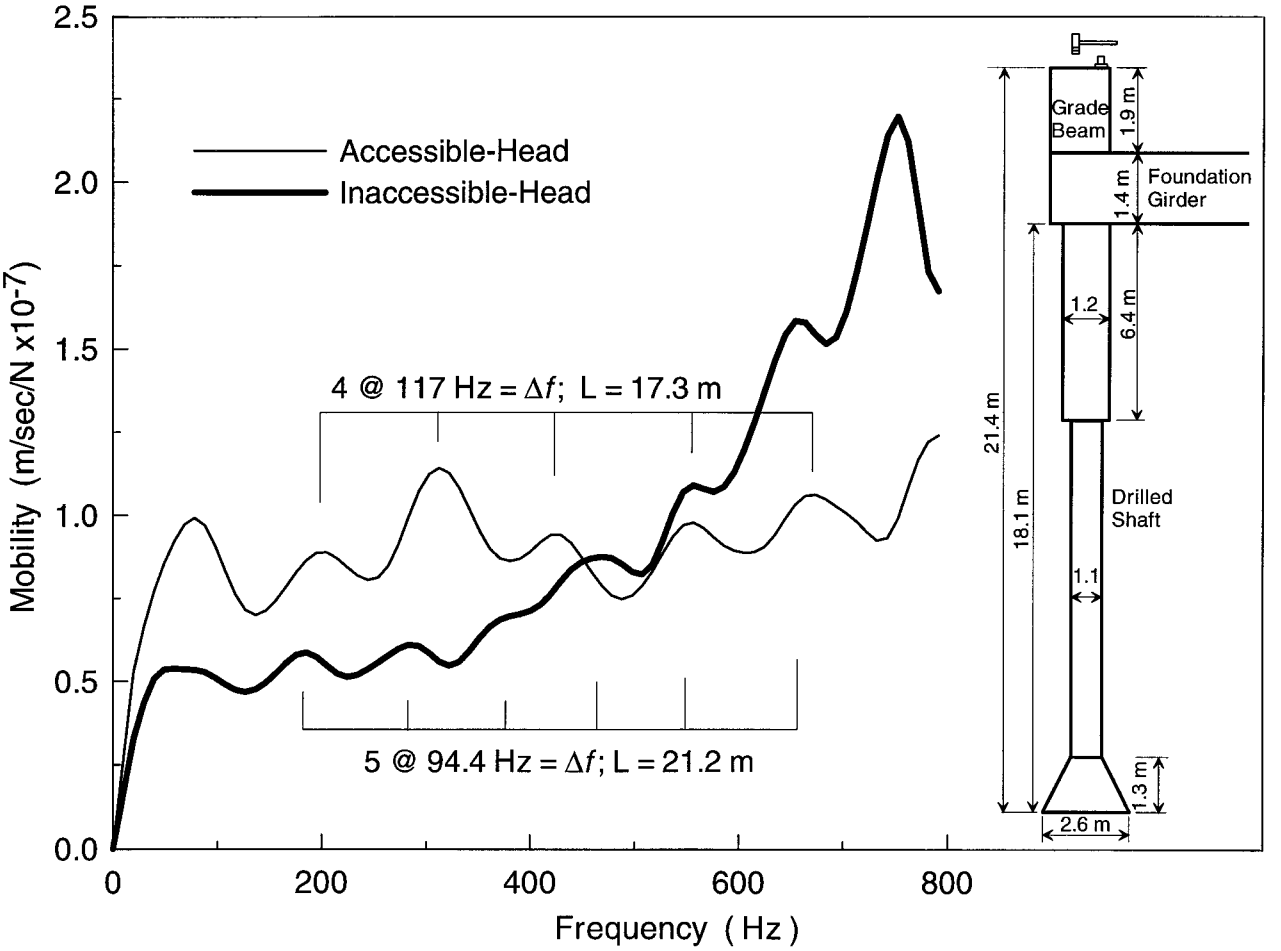

FIG. 12. Mobility Plot for Shaft 244

TABLE 4. Summary of Case Study Results

Shaft number (1)	D (m) (2)	L/D (3)	B/D (4)	A_{eff} (m^2) (5)	α_s (6)	α_t (7)	f_c^1 (Hz) (8)	f_c^2 (Hz) (9)
244	1.22	16.1	2.7	3.09	2.65	3.7	517	580
324	1.22	17.3	1	1.88	1.61	2	908	880
336	2.59	7.95	0.47	7.53	1.43	1.47	532	500
337	1.07	20.4	1.14	2.32	2.58	2.14	792	690
340	1.98	10.3	0.62	5.95	1.93	1.62	569	640
353	1.22	16.5	1	1.49	1.27	2	1,000	720
426	0.91	20.7	2.3	2.51	3.86	3.3	615	520

Note: f_c^1 = computed from (5); f_c^2 = based on differences from simulated and experimental results.

were square with the exception of shafts 244 and 426. These shafts were located below the end of a grade beam. For these shafts, A_{trib} was selected as the square of the width of the grade beam, but the F factor in (4) was taken as 0.75 to reflect the shape of the grade beam. The cutoff frequencies computed by (5) are given in the f_c^1 column. The cutoff frequencies found by comparing the experimental and simulated results are shown in the f_c^2 column. Good agreement was generally observed between the two results, as shown in Fig. 11.

Given this good agreement, the relationship given in (5) can be used to estimate the possible effectiveness of the impulse response test to identify resonances from the toe of a deep foundation for a given geometry of pile and pile cap system. This relationship is valid for concrete piles and shafts connected with a concrete pile cap.

CONCLUSIONS

The impulse response method can be used to evaluate the integrity of drilled shafts under inaccessible-head conditions when the geometry of the intervening structure does not invalidate one-dimensional wave propagation conditions in the underlying drilled shaft. The two main geometric factors that limit its applicability are the ratio of the tributary area of the intervening structure above the shaft to the area of the drilled shaft and the thickness of the pile cap to shaft diameter ratio. Based on the experimental results and numerical simulations of the drilled shafts at the NGES test site, a relation between the propagation velocity in the drilled shaft and these geometric factors was developed for concrete shafts and pile caps. This relation [(5) and Fig. 10] permits the calculation of a

cutoff frequency, above which meaningful data related to the drilled shaft cannot be extracted. Data obtained at a building site where impulse response tests were conducted on drilled shafts in both the accessible- and inaccessible-head conditions showed that the cutoff frequency relation derived on the basis of the NGES data is valid for other conditions.

ACKNOWLEDGMENTS

This work was funded by grants from the Infrastructure Technology Institute (ITI) at Northwestern University and the Federal Highway Administration (FHWA). The writers thank ITI's director, David Shultz, and Al DiMillio of FHWA for their support. The writers also thank Dr. Allen Davis of CTL and Bernie Hertlein of STS Consultants for their help in collecting the field data for the case study and for sharing their knowledge of NDE techniques.

APPENDIX I. REFERENCES

Davis, A. G. (1994). *Impedance log for the length and shape measurements of drilled shafts from mobility (TDR) tests.* STS Consultants, Inc., Northbrook, Ill.

Davis, A. G., and Dunn, C. S. (1974). ''From theory to field experience with non-destructive vibration testing of piles.'' *Proc., Inst. of Civ. Engrs.*, 2(57), 571–593.

Davis, A. G., and Robertson, S. A. (1975). ''Economic pile testing.'' *Ground Engrg.*, London, 8(3), 40–43.

Finno, R. J. (1989). ''Subsurface conditions and pile installation data: 1989 Foundation Engineering Congress test section.'' *Predicted and Observed Axial Behavior of Piles*, American Society of Civil Engineers, New York, 1–74.

Finno, R. J., and Gassman, S. L. (1998). ''Impulse response evaluation of drilled shafts.'' *J. Geotech. and Geoenvir. Engrg.*, ASCE, 123(10), 965–975.

Gassman, S. L. (1997). ''Impulse Response Evaluation of Inaccessible Foundations,'' PhD thesis, Northwestern University, Evanston, Ill.

Hearne, T. M., Reese, L. C., and Stokoe, K. H. (1981). ''Drilled-shaft integrity by wave propagation method.'' *J. Geotech. Engrg.*, ASCE, 107(10), 1327–1344.

Higgs, J. S., and Robertson, S. A. (1979). ''Integrity testing of concrete piles by shock method.'' *Concrete*, 13(10), 31–33.

Lin, Y., Sansalone, M., and Carino, N. (1991). ''Impact-echo response on concrete shafts.'' *Geotech. Testing J.*, 14(2), 121–137.

Olson, L. D., and Wright, C. C. (1989). ''Nondestructive testing of deep foundations with sonic methods.'' *Proc., Found. Engrg.: Current Principles and Practices*, F. H. Kulhawy, ed., ASCE, New York, 2, 1173–1183.

Paquet, J. (1968). ''Etude vibratoire des pieux en beton: response harmonique.'' *Annales Inst. Tech. Batim*, 21(245), 789–803 (in French).

Richart, F. E., Hall, J. R., and Woods, R. D. (1970). *Vibrations of soils and foundations.* Prentice-Hall, Englewood Cliffs, N.J.

Sansalone, M., and Carino, N. J. (1986). ''Impact-echo: a method for flaw detection in concrete using transient stress wave analysis.'' *Rep. NBSIR 86-3452*, National Bureau of Standards, Gaithersburg, Md.

Stain, R. T. (1982). ''Integrity testing.'' *Civ. Engrg.*, London, 55–59, 71–73.

APPENDIX II. NOTATION

The following symbols are used in this paper:

A = cross-sectional area of shaft (l^2);
A_{eff} = effective area of pile cap: $\pi/4(D_{\text{eff}})^2$ (l^2);
A_{trib} = tributary area of pile cap above shaft: $W_{\text{trib}} \times L_{\text{trib}}$ (l^2);
B = pile cap thickness (l);
D = diameter of shaft (l);
D_{eff} = effective diameter of pile cap (l);
E = Young's modulus of concrete (f/l^2);
f_c = cutoff frequency ($1/t$);
L = shaft length (l);
L_{trib} = tributary length of pile cap (l);
N = shaft mobility ($l/(t - f)$);
P = local maximum mobility of resonance ($l/(t - f)$);
Q = local minimum mobility of resonance($l/(t - f)$);
v_c = propagation velocity in concrete (l/t);
W_{trib} = tributary width of pile cap (l);
Δf = frequency difference between resonant peaks in mobility plot (l/t);
λ = wavelength (l); and
ρ_c = density of concrete (m/l^3).